

Copper/hexagonal Boron Nitride Nanosheet Composite as an Electrochemical Sensor for Nitrite Determination

Yu Zhang^{*}, Zhi Xia, Qianzhu Li, Guofeng Gui, Gaoyu Zhao, Shuchang Luo, Minjian Yang, Longli Lin

Key Laboratory of Applied Chemistry (Guizhou), College of Chemistry Engineering, Guizhou University of Engineering Science, Bijie 551700, PR China

*E-mail: guaiguai3522@126.com

Received: 25 January 2018 / *Accepted:* 21 March 2018 / *Published:* 10 May 2018

Hexagonal boron nitride nanosheet (h-BNNS), known as a white graphene is a promising candidate material for the fabrication of hybrid materials due to its atomically-thick sheet structure, high thermal conductivity, large surface area, unique chemical stability and thermal oxidation-resistance properties. In this paper, h-BNNS was synthesized by a hydrothermal method and then it dropped on the glassy carbon electrode (GCE) to construct h-BNNS/GCE, which has good stability because of the good film-forming ability of h-BNNS. Finally, a modified electrode (Cu-h-BNNS/GCE) was prepared by an electrodeposition technique. Due to the characteristics of h-BNNS and Cu and their synergistic effects, the modified electrode shows good electrochemical response to nitrite. The morphology and structure of the nanocomposite are studied by X-ray diffraction (XRD) and scanning electron microscopy (SEM). The electrochemical behaviors of nitrite on the as-prepared electrode were evaluated by cyclic voltammetry (CV) and differential pulse voltammetry (DPV). Under optimal conditions, the oxidation peak current of nitrite was linearly proportional to its concentration in the range from 0.09 to 9853.45 μM , with a detection limit of 0.03 μM .

Keywords: Cu metal nanoparticles; h-Boron nitride sheets; Nitrite; Electrochemical sensor

1. INTRODUCTION

Nitrite is widely present in the human environment and is the most common nitrogen-containing compound in nature. Because of its special nature, nitrite is widely used in industry and construction and it is also allowed as a limited amount in hair dyes and in meat products [1]. However, excessive intake of nitrite is harmful to humans and animals, because nitrite can interact with amines and undergo conversion into carcinogenic N-nitrosamines [2-3]. At present, numerous techniques for the highly sensitive detection of nitrite have been developed in the past few years, such as spectroscopy [4,5], chemiluminescence [6], ion chromatography and capillary electrophoresis [7,8]. Although these methods are effective, they require expensive and complicated instrumentation, highly

trained technicians, and time-consuming extraction steps. Compared with these techniques, electrochemical sensors are simple, rapid, cost-effective, and in general do not require sample pretreatment/extraction steps prior to the analysis of the desired ions in real samples.

Currently, the response mechanism of most reported nitrite sensors is based on the anodic oxidation of nitrite [9-11]. Analysis of the literature shows that anodic oxidation of nitrite can avoid interference from molecular oxygen and nitrate [12]. However, combined with the reports of Kozub et al. and the findings of our preliminary work, we determined that the anodic oxidation of nitrite on the bare glassy carbon electrode (GCE) requires a high potential, which will lead to a decrease in the anti-interference ability [13]. Thus, many different materials were used to modify the GCE to reduce the overpotential and increase the electrical response number, thereby improving the selectivity and sensitivity of the electrodes [14-16].

Hexagonal boron nitride nanosheet (h-BNNS) is a graphene-like material. For example, it has an excellent sorption capacity, good electrical insulation, an ultimate thinness, high thermal conductivity, a high surface area, and a strong resistance to oxidation, and it exhibits chemical inertness [17-19]. Although, it has drawn great attention in many fields, its use in the field of sensors is still in the nascent stage, especially in the field of direct electrocatalysis.

In this paper, h-BNNS and Cu nanocomposites were used to construct a novel electrochemical sensor for the determination of nitrite. The dispersed h-BNNS colloid was first dropped on the surface of the GCE to construct h-BNNS/GCE, which had good film-forming properties and a good electrode stability. Next, h-BNNS/GCE was immersed in a mixed solution of sulfuric acid and copper sulfate to construct a Cu-h-BNNS modified GCE by electrodeposition. The morphology and structure of the nanocomposite were studied by X-ray diffraction (XRD) and scanning electron microscopy (SEM). The main purpose of the Cu metal nanoparticles decorated on h-BNNS was to improve the sensitivity and selectivity of the modified electrode. The electrochemical behaviors of nitrite on the modified electrode were evaluated by cyclic voltammetry (CV) and differential pulse voltammetry (DPV).

2. EXPERIMENTAL

2.1 Apparatus and materials

All electrochemical experiments (CV, EIS and DPV) were carried out by a CHI660D electrochemical workstation (Shanghai Chenhua Co., China) with a three-compartment electrochemical cell, which contained a modified electrode as the working electrode, a platinum wire auxiliary electrode as the counter electrode, and a saturated calomel electrode as the reference electrode. The assembly interface was studied by scanning electron microscopy (SEM, JEOL7800F, Japan). X-ray diffraction (XRD) spectra were recorded by a DX-2700 (Dandong Gaoyuan Co., China) X-ray diffractometer with Cu K α radiation ($\lambda = 1.5406 \text{ \AA}$).

Copper sulfate, boric acid, Na₂HPO₄, KH₂PO₄, KCl and urea were obtained from Aladdin Chemical Reagents Co. Ltd. (Shanghai, China). Phosphate buffered solutions (PBS) with various pH values were prepared using 0.1 M Na₂HPO₄, 0.1 M KH₂PO₄, and 0.1 M KCl and were kept at 4 °C before use. Distilled water was used throughout this study. All other chemicals were of analytical grade and used as received without further purification.

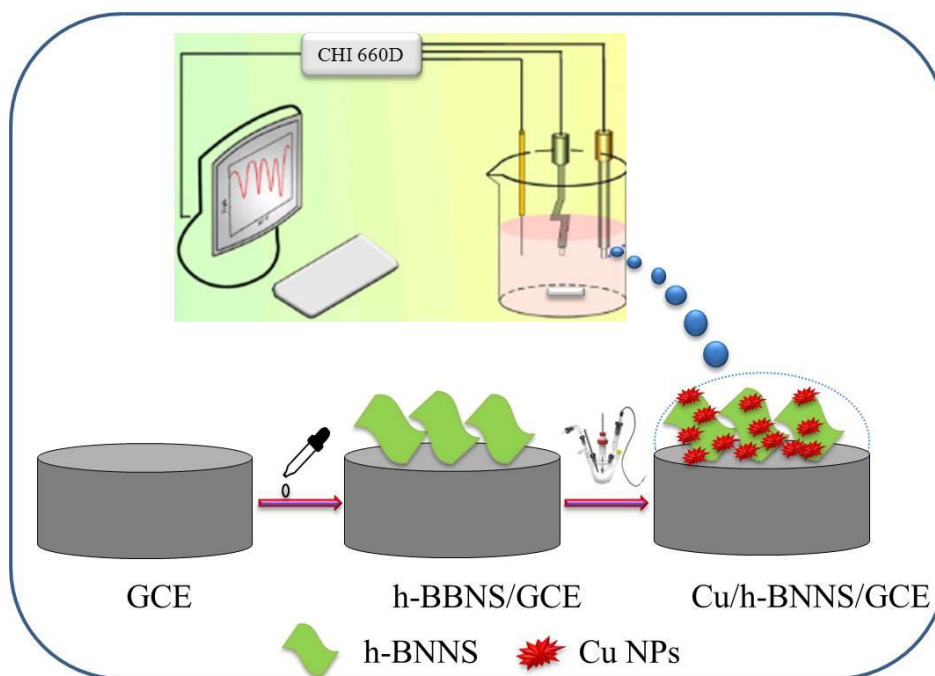
2.2 The preparation of h-BNNS

The synthesis method of h-BNNS is as follows [20]: boric acid and urea (molar ratio of 1:24) were ultrasonically dissolved in 20 mL of distilled water for 15 min, followed by drying in a vacuum oven at 60 °C. The dried mixtures were heated in a N₂ atmosphere (950 °C, 5 h), and then the white powder was sonicated in deionized water for 4 h. The resultant slurry was centrifuged at 5000 rpm for 30 min to obtain h-BNNS.

2.3 Fabrication of the proposed biosensor

The GCE was polished clean prior to the modification process. It was first polished with 0.3 and 0.05 μm alumina slurries to obtain a mirror-like surface, respectively, and then sonicated in ethanol and deionized water for several minutes and dried at room temperature.

Next, 1 mg h-BNNS was dissolved in 10 mL water by sonication to form a stable white suspension. A micro-injector was used to drop 1 μL of the suspension on the surface of the GCE. After drying at room temperature, the h-BNNS modified GCE was constructed (h-BNNS/GCE). Next, the modified electrode (h-BNNS/GCE) was immersed in a mixed solution of 1 μM copper sulfate and sulfuric acid and then electrodeposited at 0.22 V for 7 min to construct Cu-h-BNNS/GCE. The schematic illustration of the stepwise procedure of the sensor fabrication is shown in Scheme 1.



Scheme 1. The schematic illustration of the stepwise procedure of the biosensor fabrication.

2.3 Sample preparation

Simple water from the Liucang River (Bijie, Guizhou Province, China) was centrifuged at 12,000 rpm for 20 min, and then filtered through a 0.22 μm filtering membrane.

3. RESULTS AND DISCUSSION

3.1. Characterizations of h-BNNS and the modified electrode

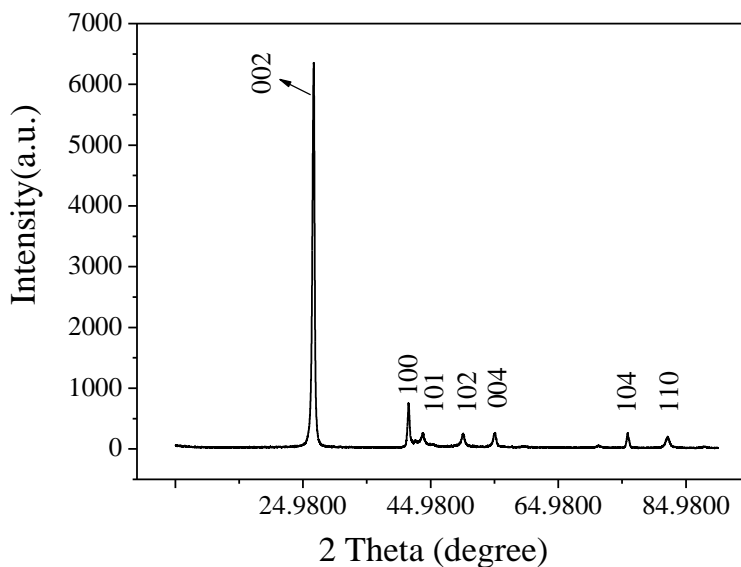


Figure 1. XRD pattern of h-BNNSs.

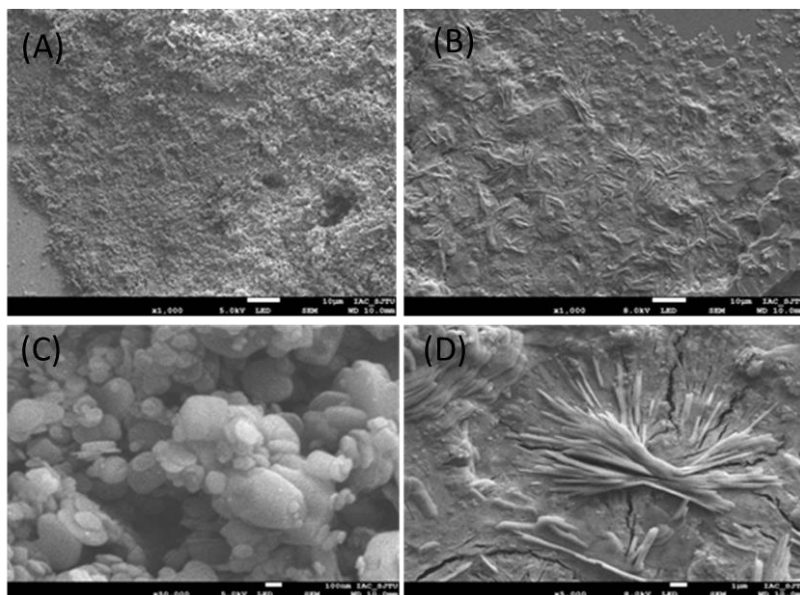


Figure 2. SEM images of h-BNNS (A, C) and Cu- h-BNNS (B, D).

Fig. 1 shows the XRD patterns for h-BNNSs. There was one a strong peak (002) and four very weak peaks (100), (101), (102), (004), (104) and (110). Compared to the hexagonal BN structure standard card (JCPDS card 34-0421), the lack of miscellaneous peaks in Fig. 1 indicates that the h-BNNSs are pure [21]. The morphologies of the different modified electrodes, including h-BNNS/GCE and Cu-h-BNNS/GCE, were studied by SEM to obtain information about the physicochemical

properties of the surfaces, and the SEM images are shown in Fig. 2. According to SEM images, h-BNNS was successfully synthesized (Fig. 2A). After dropping the suspension on the electrode, the surface of the modified electrode was porous (Fig. 2C). In addition, after the electrodeposition of copper, a bale straw-like complex formed on the surface of the electrode (Fig. 2B, Fig. 2D).

3.2. Electrochemical studies of the modified electrodes

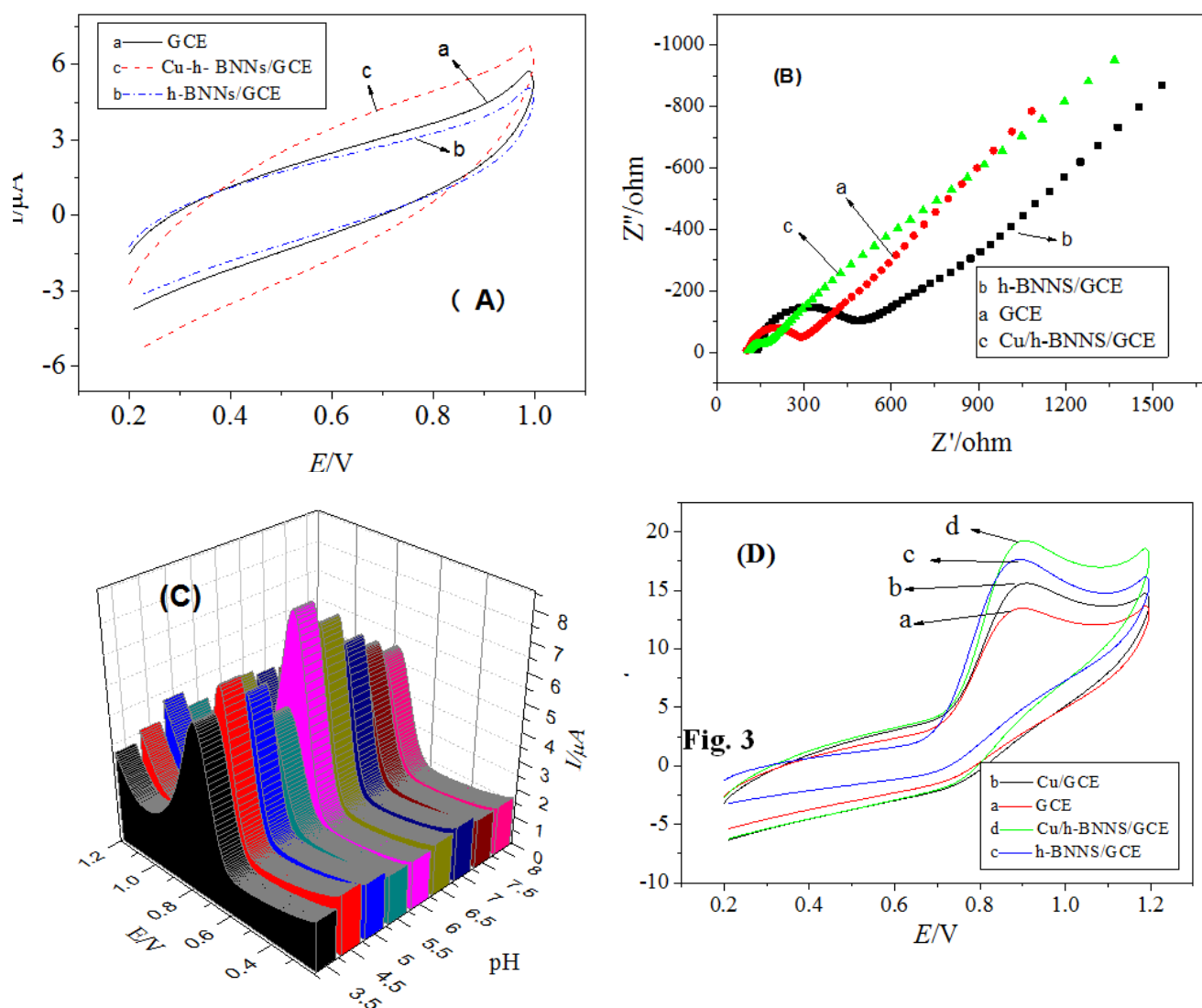


Figure 3. (A) CVs of the bare GCE (a), h-BNNS/GCE (b), Cu/h-BNNS/GCE (c) in 0.1 M PBS (pH 6.0); (B) EIS of bare GCE (a), h-BNNS/GCE (b), Cu/h-BNNS/GCE (c) in 0.1 M KCl containing 1.0 mM $[\text{Fe}(\text{CN})_6]^{4-/3-}$; (C) Effect of pH on the Cu/h-BNNS/GCE for the same concentration of NO_2^- ; (D) CVs of the bare GCE (a), h-BNNS/GCE (b), Cu/h-BNNS/GCE (c) in 0.1 M PBS (pH 6.0) containing 2 mM NO_2^- .

The stepwise assembly of the biosensor is characterized by CVs in 0.1 M pH 6.0 PBS and the results are shown in Fig. 3A. From the figure, the bare GCE (curve a) showed a slightly larger background current than the h-BNNS/GCE (curve b), indicating that the film of h-BNNS was

successfully assembled on the electrode surface. After modification with Cu (curve c), the background signal increased, and the increase is attributed to the high specific area and good electroconductivity of Cu.

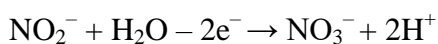
Fig. 3B illustrates the results of electrochemical impedance analysis (EIS) on the bare GCE (a), h-BNNS/GCE (b) and Cu-h-BNNS/GCE (c) in 0.1 M KCl containing 1.0 mM $[\text{Fe}(\text{CN})_6]^{4-/3-}$. The Nyquist plot contains a semicircle (R_{ct}) part at a high frequency representing the electron transfer-limited process and a linear region at a lower frequency representing the diffusion-limited process [22]. As shown in Fig. 3B, R_{ct} was calculated to be 300 Ω at the bare GCE (curve a) indicating a relatively difficult interfacial electron transfer, and when h-BNNS was added to the surface of the electrode (curve b), the R_{ct} values increased to 450 Ω . Furthermore, a small R_{ct} (approximately 100 Ω) exists at the Cu-h-BNNS/GCE (curve c), indicating fast electron transfer at the modified electrode surface. These results suggest that h-BNNS and Cu are modified successfully on the surface of the GCE and subsequently improved the conductivity.

During the experiment, the pH of the buffer solution has a great influence on the response performance of the modified electrode. In this experiment, the pH is optimized by differential pulse voltammetry (DPV). As shown in Fig. 3C, the reaction performance of the modified electrode was best when the pH value of the test solution (containing the same concentration of nitrite ions) was 6.0. Thus, PBS with a pH of 6.0 was selected in the subsequent experiments.

The electrocatalytic sensing behavior of the modified electrodes towards nitrite was investigated. Fig. 3D shows the typical CVs of different electrodes, including bare GCE (a), Cu/GCE(b), h-BNNS/GCE (c) and Cu-h-BNNS/GCE (d) in a 0.1 M PBS solution (pH= 6.0) with 2 mM NO_2^- at a scan rate of 100 mV/s. As seen from the results, the oxidation peak current of the bare GCE was the smallest. With the addition of Cu and BN, the oxidation peak currents increased. When Cu and h-BNNS were simultaneously loaded on the electrode, the oxidation peak current reached a maximum, which indicated that Cu and h-BNNS have a synergistic effect on the oxidation of NO_2^- . The favorable electrochemical response of NO_2^- further reveals that Cu and h-BNNS were compactly assembled on the surface of the electrode.

3.3. Electrochemical response of NO_2^- on the sensor

Fig. 4 shows the CV responses to the concentration of NaNO_2 . There is a good linear relationship between the concentration of NaNO_2 and the peak current. Based on the results, the Cu-h-BNNS/GCE can electively catalyze the nitrite oxidation reaction. DPV obtained at the Cu-h-BNNS/GCE in 0.1 M PBS (pH= 6.0) containing different concentrations of NaNO_2 are shown in Fig. 5. Clearly, with the addition of NaNO_2 , the oxidation peak currents gradually increased, suggesting that NaNO_2 was oxidized. The reaction mechanism was as follows [23,29]:



The inset represents the corresponding linear relationship between the peak current and the NaNO_2 concentration.

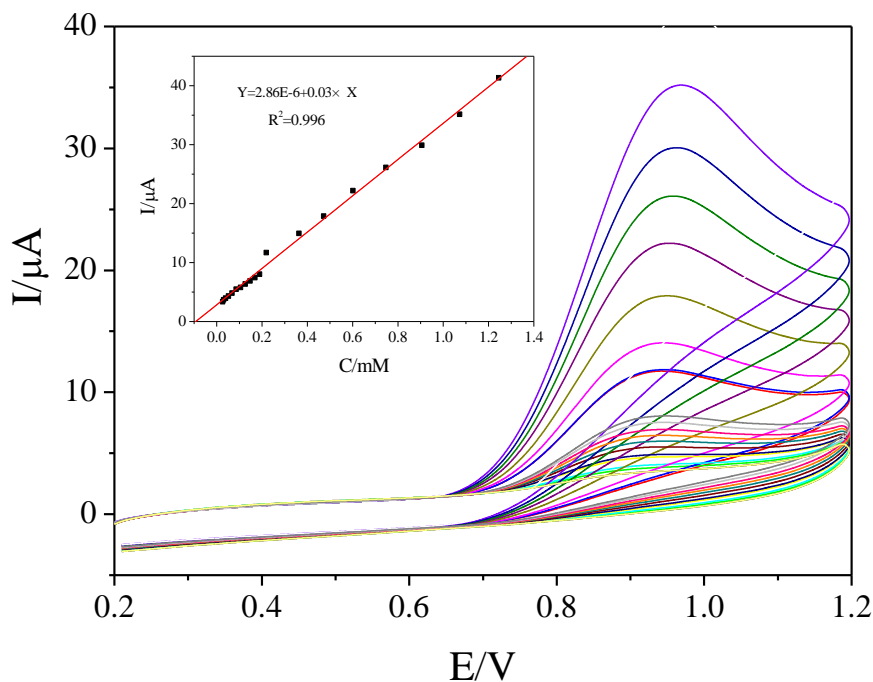


Figure 4. CVs of the Cu/h-BNNS/GCE before and after the addition of NO_2^- . (Inset shows the plot of current vs. the concentration of NO_2^- . Scan rate: 100 mV/s).

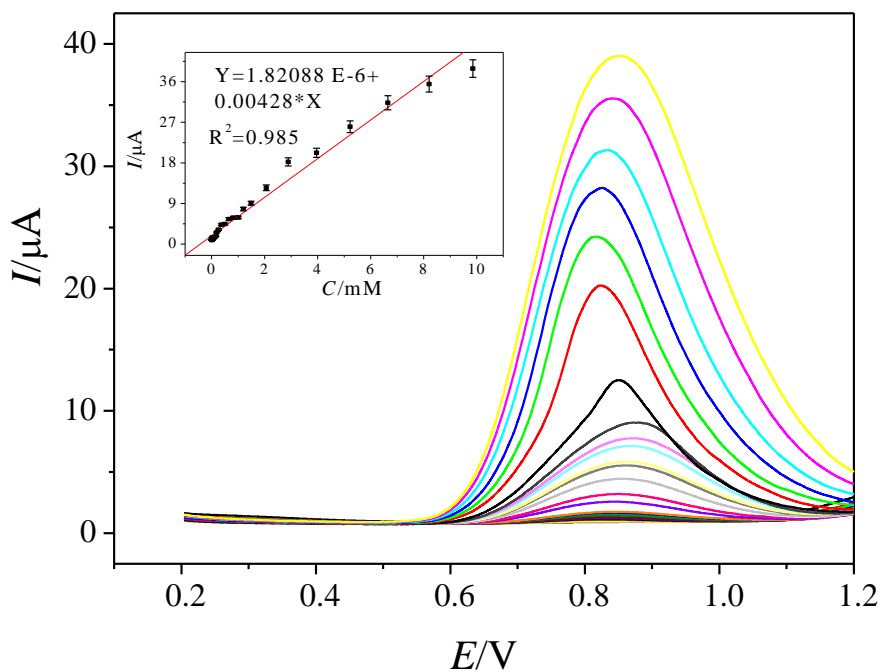


Figure 5. DPVs for NO_2^- in the concentrations range of 0.09 to 9853.45 μM (Inset shows the corresponding calibration plot).

The results show that the peak current is proportional to the concentration of NaNO_2 ranging from 0.09 to 9853.45 μM . The linear regression equation of the former is $Y = 1.82\text{E-}6 + 0.004X$, with a correlation coefficient of 0.985. The limit of detection (LOD) was determined to be ($S/N=3$) 0.03 μM . These results demonstrate that Cu-h-BNNS/GCE can be employed to sensitively monitor nitrite concentrations. The obtained results from this modified electrode were compared with other nitrite sensors (Table 1). The contrast results show that in most of nitrite sensors using copper as a catalyst, our sensor has better performance in detection limit and linear range, which indicates that BNNS has played a very important role, and BNNS has great potential for the construction of other sensors. Comparison of other metal nanocomposites, the performance of Cu-h-BNNS is also good.

Table 1. Compared with diverse nitrite sensors

Modified electrode	Linear range (μM)	Detection limit (μM)	Applied potentials (V) (vs. SCE)	Reference
^a CoL/MNSs/CPE	0.2–30.0	0.015	0.95	[12]
^b Pd/Fe ₃ O ₄ /polyDOPA/RGO	2.5–6470	0.5	0.82	[15]
^c Pt/Ni(OH) ₂ /MWCNTs/GCE	0.4–5670	0.13	0.75	[16]
^d Co ₃ O ₄ /RGO	1–380	0.14	0.55	[22]
^e Cu-NDs/RGO	1.2–13000	0.4	-0.2	[24]
^f Au/Cu-MOF/CPE	0.05–717	0.03	0.8	[25]
^g Ag/Cu/MWCNTs/GCE	1.0–1000	0.2	0.85	[26]
^h Cu/MWCNTs/RGO/GCE	0.1–75	3.0	-0.25	[27]
ⁱ Cu-MHA-EDA/CPE	0–0.01	1.46	1.0	[28]
^j Cu/BNNS/GCE	0.09–9853.45	0.03	0.85	This work

^a cobalt(II)-Schiff base complex/magnetite nanospheres

^b Pd/Fe₃O₄/ 3,4-Dihydroxy-l-phenylalanine/reduced graphene oxide

^c Pt/Ni(OH)₂/Multi-walled carbon nanotubes/GCE

^d Co₃O₄/reduced graphene oxide

^e Copper nanodendrites/reduced graphene oxide

^f Au/Cu metal-organic framework/carbon paste electrode

^g Au/Cu/ Multi-walled carbon nanotubes/GCE

^h Cu/ Multi-walled carbon nanotubes/reduced graphene oxide/GCE

ⁱ copper (II)-modified humic acids complexes-ethylenediamine/carbon paste electrode

3.4. Interference, reproducibility and stability study

In the real samples, there is not only nitrite but also other coexisting ions, such as Cl^- , Na^+ , K^+ , Ca^{2+} , Mg^{2+} , Zn^{2+} and NO_3^- . To investigate the selectivity of the studied electrode to nitrite, an interference experiment was carried out at the Cu-h-BNNS modified electrode by adding different foreign species into a stirred 0.1 M PBS (pH 6.0, containing 0.2 mM NO_2^-). No obvious interference was observed when NaNO_3 , CaCl_2 , KCl , MgSO_4 , and ZnCl_2 with 50-fold higher concentrations were added, which indicates that the Cu-h-BNNS/GCE has good anti-interference ability and selectivity.

The reproducibility and stability are also the important performance factors in analytical applications. The Cu-h-BNN/GCE was suspended above a 0.1 M pH 6.0 PBS at 4 °C. The current

response to the same concentration of NO_2^- was measured daily. After a week, the modified electrode retained 91% of its initial response. The fabrication reproducibility of six electrodes, made independently, showed an acceptable repeatability with the an R.S.D. of 5.4%. Therefore, the modified electrode has good stability and excellent repeatability, and it was suitable for continual operation.

3.5. Real sample analysis

To determine the feasibility of analysis of real samples, the prepared sensor was used to detect nitrite in river water (Liucang River, Bijie City). The results are shown in Table 2. The recoveries were in the range of 98.3%–117.7%, suggesting that the fabricated sensor could be used practically for the routine analysis of nitrite in real applications.

Table 2. Determination of nitrite in real samples.

Samples	Added / $\mu\text{mol}\cdot\text{L}^{-1}$	Found ^a / $\mu\text{mol}\cdot\text{L}^{-1}$	Recovery/%
1	20.00	23.54±0.2	117.7
2	20.00	22.47±0.3	112.4
3	20.00	19.65±0.2	98.3

^a Mean ± SD of three measurements.

4. CONCLUSION

In summary, a novel electrochemical sensor for the determination of nitrite based on bale straw-like Cu-h-BNNS was successfully constructed. Cu-h-BNNS possessed enhanced electrocatalytic activity and high reliability, which can be attributed to the synergetic effect between the CuNPs and h-BNNS. The special structures of Cu-h-BNNS provide a large surface area, more active sites and a high electrical conductivity. Under optimal conditions, the developed electrochemical sensor for nitrite assays displayed superior analytical performance, such as good a selectivity, excellent reproducibility, a wide linear range (0.09 to 9853.45 μM) and a low limit of detection (0.03 μM). The recovery experiment shows that the proposed method is promising for the determination and monitoring of nitrite in water and food samples.

ACKNOWLEDGMENTS

The Joint Foundation Project of Guizhou Province, Bijie City and Guizhou University of Engineering Science (LH[2015]7587, LH[2015]7588, LH[2016]7056 and LH[2016]7058), The Department Education Project of Guizhou Province (KY[2015]450), The Science and Technology Bureau Project of Bijie City ([2016]21) and Chemical Engineering Experimental Teaching Demonstration Center of Guizhou Province, Key disciplines of Applied Chemistry and chemical engineering and Technology in Guizhou Province supported this work. The authors are grateful for the referee's helpful comments on the manuscript.

References

1. Z.H. Dai, H.Y. Bai, M. Hong, Y.Y. Zhu, J.C. Bao, J. Shen, *Biosens. Bioelectron.*, 23 (2008) 1869.
2. M. Pietrzak, M.E. Meyerhoff, *Anal. Chem.*, 81 (2009) 3637.
3. D. Ning, H. F. Zhang, J. B. Zheng, *J. Electroanal. Chem.*, 717 (2014) 29.
4. H. Takiguchi, A. Tsubata, M. Miyata, T. Odake, H. Hotta, T. Umemura, K. Tsunoda, *Anal. Sci.*, 22 (2006) 1017.
5. J.Y. Ma, H. Yao, H.Q. Yu, L.S. Zuo, H.Y. Li, J.G. Ma, Y.R. Xu, J. Pei, X.Y. Li, *Chem. Eng. J.*, 335 (2018) 401.
6. A. Lagalante, P. Greenbacker, *Anal. Chim. Acta*, 590 (2007) 151.
7. Aneta Antczak-Chrobot, Paulina Bąk, Maciej Wojtczak, *Food. Chem.*, 240 (2018) 648.
8. X. Wang, E. Adams, A. V. Schepdael, *Talanta*, 97 (2012) 142.
9. H. Wu, S. Fan, X. Jin, H. Zhang, H. Chen, Z. Dai, X. Zou, *Anal. Chem.*, 86 (2014) 6285.
10. P. Chen, A.W. Zhao, J. Wang, Q.Y. He, H.G. Sun, D.P. Wang, M. Sun, H.Y. Guo, *Sens. Actuators B-Chem.*, 256 (2018) 107.
11. L.B. Li, D. Liu, K. Wang, H.P. Mao, T.Y. You, *Sens. Actuators B-Chem.*, 252 (2017) 17.
12. M. Parsaei, Z. Asadi, S. Khodadoust, *Sens. Actuators B-Chem.*, 220 (2015) 1131.
13. B. R. Kozub, N. V. Rees, R. G. Compton, *Sens. Actuators B-Chem.*, 143 (2010) 539.
14. H. Bagheri, A. Hajian, M. Rezaei, A. Shirzadmehr, *J. Hazardous Materials*, 324 (2017) 762.
15. Z.Y. Zhao, Z.H. Xia, C.Y. Liu, H. Huang, W.H. Ye, *Electrochim. Acta*, 256 (2017) 146.
16. Q.L. Sheng, D. Liu, J.B. Zheng, *J. Electroanal. Chem.*, 796 (2017) 9.
17. Y. Yao, Z. Lin, Z. Li, X. Song, K.S. Moon, C.P. Wong, *J. Mater. Chem.*, 22 (27) (2012) 13494.
18. Y. Lin, C.E. Bunker, K.A. Fernando, J.W. Connell, *ACS Appl. Mater. Interfaces*, 4 (2012) 1110.
19. G.H. Yang, J.J. Shi, S. Wang, W.W. Xiong, L.P. Jiang, C. Burda, et al., *Chem. Commun.*, 49 (2013) 10757.
20. A. Nag, K. Raidongia, K.P. Hembram, R. Datta, U.V. Waghmare, C.N. Rao, *ACS Nano* 4 (3) (2010) 1539.
21. Y. Kubota, K. Watanabe, O. Tsuda, T. Taniguchi, *Science*, 317 (5840) (2007) 932.
22. Y. Haldorai, J.Y. Kim, A.T. Ezhil Vilian, N.S. Heo, Y.S. Huh, Y.K. Han, *Sens. Actuators B-Chem.*, 227 (2016) 92.
23. P. Wang, M.Y. Wang, F.Y. Zhou, G.H. Yang, L.L. Qu, X.M. Miao, *Electrochem. Commun.*, 81 (2017) 74.
24. D. Zhang, Y.X. Fang, Z.Y. Miao, M. Ma, X. Du, S. Takahashi, J. Anzai, Q. Chen, *Electrochim. Acta*, 107 (2013) 656.
25. B.Q. Yuan, J.C. Zhang, R.C. Zhang, H.Z. Shi, N. Wang, J.W. Li, F.J. Ma, D.J. Zhang, *Sens. Actuators B-Chem.*, 222, (2016) 632.
26. Y. Zhang, J. Nie, H. Wei, H. Xu, Q. Wang, Y. Cong, J. Tao, Y. Zhang, L. Chu, Y. Zhou, X. Wu, *Sens. Actuators B-Chem.*, 258 (2018) 1107.
27. H. Bagheri, A. Hajian, M. Rezaei, A. Shirzadmehr, *J. Hazardous Materials*, 324 (2017) 762.
28. C.A. Ramdane-Terbouche, A. Terbouche, S. Djebbar, D. Hauchard, *Talanta*, 119 (2014) 214.